PEPPo universal access to polarized positrons

D. Abbott,[1] P. Adderley,[1] A. Adeyemi,[3] P. Aguilera,[1] M. Ali,[1] H. Areti,[1] M. Baylac,[2] J. Benesch,[1] G. Bosson,[2] B. Cade,[1] A. Camsonne,[1] L. Cardman,[1] J. Clark,[1] P. Cole,[4] S. Covert,[1] C. Cuevas,[1] O. Dadoun,[5] D. Dale,[4] H. Dong,[1] J. Dumas,[1,2] E. Fanchini,[2] T. Forest,[4] E. Forman,[1] A. Freyberger,[1] E. Froidefond,[2] S. Golge,[6] J. Grames,[1] P. Guèye,[3] J. Hansknecht,[1] P. Harrell,[1] J. Hoskins,[10] C. Hyde,[7] B. Josey,[13] R. Kazimi,[1] Y. Kim,[1,4] D. Machie,[1] K. Mahoney,[1] R. Mammei,[1] M. Marton,[2] J. McCarter,[11] M. McCaughan,[1] M. McHugh,[14] D. McNulty,[4] T. Michaelides,[1] R. Michaels,[1] B. Moffit,[1] C. Muñoz Camacho,[8] J.-F. Muraz,[2] K. Myers,[9] A. Opper,[14] M. Poelker,[1] J.-S. Réal,[2] L. Richardson,[1] S. Setiniyaz,[4] M. Stutzman,[1] R. Suleiman,[1] C. Tennant,[1] C. Tsai,[12] D. Turner,[1] M. Ungaro,[1] A. Variola,[5] E. Voutier,[2,8] Y. Wang,[1] and Y. Zhang[9]

(PEPPo Collaboration)

[1] *Thomas Jefferson National Accelerator Facility, Newport News, VA 23606, USA*
[2] *LPSC, Université Grenoble-Alpes, CNRS/IN2P3, 38026 Grenoble, France*
[3] *Hampton University, Hampton, VA 23668, USA*
[4] *Idaho State University, Pocatello, ID 83209, USA*
[5] *LAL, Université Paris-Sud & Université Paris-Saclay, CNRS/IN2P3, 91898 Orsay, France*
[6] *North Carolina Central University, Durham, NC 27707, USA*
[7] *Old Dominion University, Norfolk, VA 23529, USA*
[8] *IPN, Université Paris-Sud & Université Paris-Saclay, CNRS/IN2P3, 91406 Orsay, France*
[9] *Rutgers, The State University of New Jersey, Piscataway, NJ 08854, USA*
[10] *The College of William & Mary, Williamsburg, VA 23187, USA*
[11] *University of Virginia, Charlottesville, VA 22901, USA*
[12] *Virginia Polytechnique Institut and State University, Blacksburg, VA 24061, USA*
[13] *University of New Mexico, Albuquerque, NM 87131, USA*
[14] *The George Washington University, Washington, DC 20052, USA*

The Polarized Electrons for Polarized Positrons experiment at the injector of the Thomas Jefferson National Accelerator Facility has demonstrated for the first time the efficient transfer of polarization from electrons to positrons produced by the polarized bremsstrahlung radiation induced by a polarized electron beam in a thick target. Polarization transfer as high as 80% has been measured for an initial electron beam momentum of 8.19 MeV/c . This technique expands polarized positron capabilities to GeV to MeV electron beams, and opens access to polarized positron beam physics to a wide Community.

PACS numbers: 29.27.Hj, 41.75.Fr, 13.88.+e

Positron beams, both polarized and unpolarized, with energies ranging from a few eV to hundreds of GeV are unique tools for the study of the physical world. For energies up to several hundred keV, they allow the study of surface magnetization properties [1] of materials and their inner structural defects [2]. In the several to tens of GeV energy range, they provide the complementary experimental observables essential for an unambiguous understanding of the nucleon structure [3]. In the several hundreds of GeV energy range, they are considered essential for the next generation of experiments that will search for physics beyond the Standard Model [4]. Unfortunately, the creation of polarized positron beams has been very difficult. Radioactive sources can be used for low energy positrons [5], but the flux is very restricted. While storage ring facilities can rely on the natural build-up of polarization from the Sokolov-Ternov effect [6], external beams and continuous wave facilities require different scenarios. These new schemes rely on the polarization transfer in the e^+e^--pair creation process from circularly polarized photons [7, 8], but use different methods to produce the polarized photons.

Two alternative production techniques have been investigated successfuly: the Compton backscattering of a polarized laser from a GeV electron beam [9], and the synchrotron radiation of a multi-GeV electron beam travelling within a helical undulator [10]. Both demonstration experiments reported high positron polarization, supporting the efficiency of the pair production process for producing a polarized positron beam. However, these techniques require high energy electron beams and challenging technologies that intrinsically limit their range of applications.

A novel approach, which we refer to as the Polarized Electrons for Polarized Positrons (PEPPo) concept [11, 12], has been investigated at the Continuous Electron Beam Accelerator Facility (CEBAF) of the Thomas Jefferson National Accelerator Facility (JLab). Taking advantage of advances in high polarization, high intensity electron sources [13], it uses the polarized photons generated by the bremsstrahlung radiation of low energy longitudinally polarized electrons within a tungsten

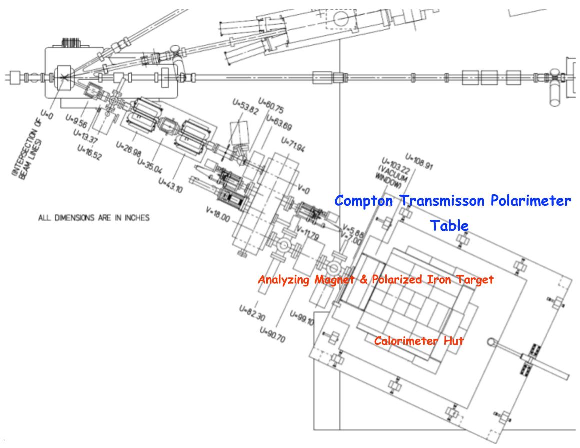

FIG. 1. Schematic of the PEPPo line and apparatus.

target to produce polarized e^+e^--pairs. It is expected that the PEPPo concept can be developed efficiently with a low energy, high intensity, and high polarization electron beam driver, opening access to polarized positron beams for a wide community.

The PEPPo experiment [14] was designed to evaluate the PEPPo concept for a polarized positron source by measuring the polarization transfer from primary electron beam to the produced positrons. We constructed a new beam line (Fig. 1) at the CEBAF injector [15] where polarized electrons up to 8.19 MeV/c were transported to a 1 mm thick tungsten positron production target (T1) followed by a positron collection, selection, and characterization system [16]. Longitudinally polarized electrons interacting at T1 radiate elliptically polarized photons whose circular component (P_γ) is proportional to the electron beam polarization (P_e). Within the same target, polarized photons produce polarized e^+e^--pairs whose perpendicular ($P_\perp$) and longitudinal ($P_\parallel$) polarization components are both proportional to P_γ and therefore P_e. However, the azimuthal average cancels $P_\perp$ contribution such that the secondary e^+-beam is essentially longitudinally polarized. Immediately after T1, a short focal length solenoid lens (S1) collects and guides the positrons to a D$\overline{\text{D}}$ spectrometer with two 90° bend dipoles selecting a ##% momentum slice. A second solenoid lens (S2) at the exit of the spectrometer collects and transports the selected positrons to a polarimeter. This polarimeter [16] begins with a 2 mm densimet (90.5%W+7%Ni+2.5%Cu) conversion target (T2) followed by a 7.5 cm long, 5 cm diameter iron cylinder centered in a solenoid that saturates and polarizes the iron core. Following the procedure of Ref. [16], the average longitudinal polarization was determined $< P_T >= 7.06 \pm 0.09\%$ in very good agreement with previsouly reported value [16]. An electromagnetic calorimeter with 9 CsI crystals ($6{\times}6{\times}28$ cm^3) arranged in a 3×3-array is placed at the exit of the polarimeter solenoid. Polarized positrons convert at T2 via bremsstrahlung and annihilation processes into polarized photons whose polarization orientation and magnitude depend on the positron polarization. Because of the polarization dependence of the Compton process, the number of photons passing through the iron core and subsequently detected by the CsI-array depends on the relative orientation of the photon and iron core polarizations. Comparing the signals delivered by each crystal for reversed magnet polarities and same positron polarization, or fixed magnet polarity and reversed positron polarization orientation resulting from reversed intial electron beam polarization, one measures the experimental Compton asymmetry

$$A_C^p = P_\parallel \, P_T \, A_p = \epsilon_P \, P_e \, P_T \, A_p = \epsilon_P \, P_e \, P_T \, k_A A_e \quad (1)$$

where $A_p(e)$ is the $e^{+(-)}$ analyzing power of the polarimeter, ϵ_P is the electron-to-positron polarization transfer efficiency, and k_A is the positron-to-electron analyzing power scaling factor. PEPPo measured the momentum dependence of ϵ_P for p_e=8.19±0.04 MeV/c electrons over a positron momentum range of 3.02 to 6.25 MeV/c.

The apparatus was calibrated by using the electron beam (with independently measured momentum and polarization [15]) at each selected positron momentum, then the fields were reversed for the positron measurements. The experimentally determined S1, D$\overline{\text{D}}$, and S2 currents associated with the beam setup compared satisfactorily to the G4PEPPo model of the PEPPo experiment worked out within the GEANT4 framework [17]. The electron beam polarization was measured at 5.34±0.02 MeV/c with a Mott polarimeter [15]: P_e=83.7 ± 0.6 ± 2.8%, where the first uncertainty is statistical and the second is systematic and comes from the theoretical determination and extrapolation of the Mott polarimeter analyzing power.

Electrons arriving at T2 convert into photons that are detected in the crystal array read by photomultipliers (PMT). The effective gain of each crystal was calibrated prior to beam exposure with ^{137}Cs and ^{22}Na radioactive sources, and monitored during data taking by controlling the position of the 511 keV peak produced by the annihilation of positrons created in the iron core. This method insures a robust and stable energy measurement, intrinsically corrected for possible radiation damage or PMT-aging effects. A positron trigger was formed from a coincidence between the central crystal (C5) and a 1 mm thick scintillator (TS) placed between the PEPPo line vacuum exit window and T2; it constitutes an effective charged particle trigger that considerably reduces the neutral background into the crystal array. The electronic readout operated in two modes: single event mode; and integrated mode in which the PMT signal from the crystal was integrated over the total time associated with a fixed beam polarization orientation (helicity gate). This mode was used in high rate background-free situations (particularly for electron calibration measurements). The comparison of the total energy deposit ($E^{\pm}(\lambda, h)$) during the helicity gate for each beam polarization orientation and fixed analyzing magnet polarity (λ=$\pm$1) gives the experimental asymmetry where h=$\pm$1 indicates the beam helicity status at the electron source, that can be reversed inserting a half-wave plate on the excitation laser light pathway [15]. Data taking was repeated for each magnet polarity and beam helicity, and the results were combined statistically to provide the actual Compton asymmetries A_C^e for electrons, free from eventual false asymmetries related to the beam or the analyzing magnet.

$$A_C^e = P_e \, P_T \, A_e \, . \tag{2}$$

Experimental values reported in Tab. I feature high statistical accuracy (< 1%) and same order systematic errors originating from the determination of the pedestal signal. Since the beam and target polarizations were known, these constitute measurements of A_e (Eq. 2); they show the expected order-of-magnitude increase with electron momentum (Fig. 2).

Positron data were recorded on an event-by-event basis and, because of the trigger configuration, involve only C5. The experimental information consists of the energy deposited in C5 and the coincidence time (t_c) between TS and C5. The energy yield $Y_{\lambda h}^{\pm}$ was constructed for each λh configuration

$$Y_{\lambda h}^{\pm} = \sum_{ij} \frac{\left(N_{m,ij}^{\pm}(\lambda, h) - N_{r,ij}^{\pm}(\lambda, h) \right) \, \mathcal{E}_{ij}}{Q_i^{\pm} \, dt_i^{\pm}} \tag{3}$$

where the sums run over the helicity gates (i) and the events (j) occuring during each gate; $N_{m,ij}^{\pm}$ is the number of events within a selected time window around the t_c peak; $N_{r,ij}^{\pm}$ is the random coincidences contamination deduced from a fit of the global t_c spectra; $\mathcal{E}_{ij}$ is the energy deposited in C5, $Q_i^{\pm}$ is the helicity gate beam charge determined from a beam current monitor on the main accelerator line, and $dt_i^{\pm}$ represents the electronics and data acquisition dead-time correction measured with specific helicity gated scalers. The combination of each λh configurations provides the Compton asymmetries A_C^p (Eq. 1). Tab. I reports experimental asymmetries and uncertainties for each positron momentum, insuring a mimimum energy deposit $\mathcal{E}_{ij} > 511$ keV. Main sources of systematics originate from the energy calibration procedure, the random subtraction method, and the selection of coincidence events. They are quadratically combined to deliver Tab. I values whose dominant contributions are random subtraction effects.

The complete PEPPo beam line, magnetic environment, and detection system was modeled within G4PEPPo, taking advantage of previous efforts implementing in GEANT4 the description of polarization phenomena in electromagnetic processes [18, 19]. The calibration of the analyzing power of the polarimeter relies on the comparison between experimental and simulated electron asymmetries. It allows to benchmark GEANT4 physics packages and resolves related systematic uncertainties within the limits of the measurement accuracy. The excellent agreement between electron measurements and simulations (Fig. 2) indicates an accurate understanding of the PEPPo line optics and the quality of the operation of the polarimeter. The positron analyzing power A_p (Fig. 2) is deduced from calibrated G4PEPPo illuminating the polarimeter with a secondary e^+-beam determined from the optic properties of the PEPPo line. Because of the actual large e^+-beam size at T2, this procedure does not bring any significant additional systematics. The combination of the supplementary e^+-to-γ annihilation conversion process together with the minimum energy deposit requirement leads to $k_A > 1$ (Tab. I). The latter effect is strong at low e^+ momenta where it removes a significant part of the energy spectra acting as a dilution of the polarization sensitivity.

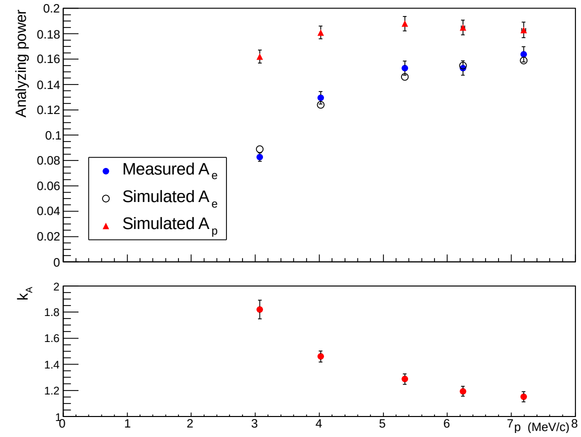

FIG. 2. Electron and positron analyzing powers of the central crystal of the polarimeter (top panel), together with the simulated positron-to-electron analyzing power scaling factor (bottom panel). Statistical uncertainties were combined quadratically with systematic uncertainties taken from P_e, P_T, and A_C^e to determine acutal error bars.

The positron longitudinal polarization $P_{\parallel}$ (Eq. 1) and the polarization transfer efficiency

$$\epsilon_P = \frac{1}{k_A} \frac{A_C^p}{A_C^e} \tag{4}$$

as obtained independently of P_e and P_T, are reported in Tab. I, and compared on Fig. 3 with GEANT4 model expectations. The current data show large positron polarization ($P_{\parallel} > 40\%$) and polarization transfer efficiency ($\epsilon_P > 50\%$) over the explored momentum range. The bremsstrahlung of longitudinally polarized electrons is

TABLE I. PEPPo electron and positron measurements and polarization data at the central C5 crystal.

Momentum		Experimental asymmetries						Analyzing power scaling factor			Polarization data					
p	δp	A_C^e	$\delta A_C^{e\,Sta.}$	$\delta A_C^{e\,Sys.}$	A_C^p	$\delta A_C^{p\,Sta.}$	$\delta A_C^{p\,Sys.}$				ϵ_P	$\delta\epsilon_P^{Sta.}$	$\delta\epsilon_P^{Sys.}$	$P_\parallel$	$\delta P_\parallel^{Sta.}$	$\delta P_\parallel^{Sys.}$
(MeV/c)	(MeV/c)	(‰)	(‰)	(‰)	(‰)	(‰)	(‰)	k_A	$\delta k_A^{Sta.}$	$\delta k_A^{Sys.}$	(%)	(%)	(%)	(%)	(%)	(%)
3.07	0.01	4.89	0.03	0.07	7.03	1.10		1.82	0.06	0.04						
4.02	0.02	7.65	0.05	0.07	8.71	0.49		1.46	0.02	0.04						
5.34	0.02	9.03	0.03	0.03	11.4	0.5		1.29	0.02	0.04						
6.25	0.03	9.04	0.04	0.04	12.0	0.4		1.19	0.02	0.04						
7.19	0.03	9.68	0.04	0.05				1.15	0.02	0.04						

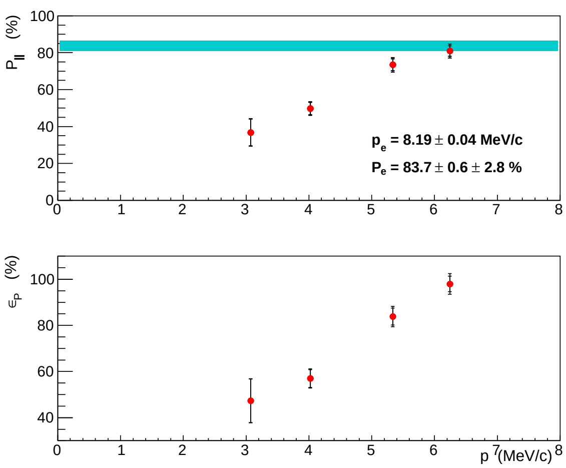

FIG. 3. PEPPo measurements of the positron polarization (top panel) and polarization transfer efficiency (bottom panel); statistics and systematics are reported for each point, and the shaded area indicates the electron beam polarization.

therefore demonstrated as an efficient process to generate longitudinally polarized positrons. Agreement between measurements and expectations further suggests that the dominant production mechanism for thick targets is a two-step process where pair creation follows electron beam bremsstrahlung i.e. one-step virtual pair production mechanisms don't seem significant for e^--to-e^+ polarization transfer within thick targets.

PEPPo demonstrated longitudinal polarization transfer as high as 80% from 8.19 MeV/c electrons to positrons, expanding the possibilities for the production of high intensity polarized positron beams from GeV accelerators to MeV beams. These results can be extrapolated to any initial electron beam energy above the pair production threshold, depending on the desired positron flux and polarization. The low magnitude of the required minimum electron energy opens a large field of applications ranging from thermal polarized positron facilities to high energy colliders.

We are deeply grateful to the SLAC E-166 Collaboration, particularly K. Laihem, K. McDonald, S. Riemann, A. Schälicke, P. Schüler, J. Sheppard and A. Stahl for loan of fundamental equipment parts and support in GEANT4 modeling. We also thank N. Smirnov for delivery of critical hardware. This work was supported in part by the U.S. Department of Energy, the French Centre National de la Recherche Scientifique, and the International Linear Collider project. Jefferson Science Associates operates the Thomas Jefferson National Accelerator Facility under DOE contract DE-AC05-06OR23177.

[1] R. W. Gidley, A. R. Köymen, and T. W. Capehart, Phys. Rev. Lett. **49**, 1779 (1982).
[2] R. Krause-Rehberg and H. S. Leipner, *Positron Annihilation in Semi-conductors* (Springer-Verlab Berlin Heidelberg, 1999).
[3] E. Voutier, in *Nuclear Theory*, Vol. 33, edited by A. I. Georgievia and N. Minkov (Heron Press, Sofia, 2014) p. 142.
[4] T. Behnke, J. E. Brau, B. Foster, J. Fuster, M. Harrison, J. M. Paterson, M. Peskin, M. Stanitzki, N. Walker, and H. Yamamoto, *The International Linear Collider Technical Design Report*, Executive summary 1 (2013).
[5] P. W. Zitzewitz, J. C. V. House, A. Rich, and D. W. Gidley, Phys. Rev. Lett. **43**, 1281 (1979).
[6] A. A. Sokolov and I. M. Ternov, Sov. Phys. Dokl. **8**, 1203 (1964).
[7] H. Olsen and L. Maximon, Phys. Rev. **114**, 887 (1959).
[8] E. A. Kuraev, Y. Bistritskiy, M. Shatnev, and E. Tomasi-Gustafsson, Phys. Rev. C **81**, 055208 (2010).
[9] T. Omori *et al.*, Phys. Rev. Lett. **96**, 114801 (2006).
[10] G. Alexander *et al.*, Phys. Rev. Lett. **100**, 210801 (2008).
[11] E. G. Bessonov and A. A. Mikhailichenko, in *EPAC96* (1996) p. THP071L.
[12] A. P. Potylitsin, Nucl. Inst. Meth. A **398**, 395 (1997).
[13] P. Adderley *et al.*, Phys. Rev. ST Acc. Beams **13**, 010101 (2010).
[14] J. Grames, E. Voutier, *et al.*, *Polarized electrons for polarized positrons: a proof-of-principle experiment*, Experiment **E12-11-105** (Jefferson Laboratory, Newport News, Virginia, 2012).
[15] R. Kazimi *et al.*, in *EPAC04* (2004) p. TUPLT164.
[16] G. Alexander *et al.*, Nucl. Inst. Meth. A **610**, 451 (2009).
[17] S. Agostinelli *et al.*, Nucl. Inst. Meth. A **506**, 250 (2003).
[18] R. Dollan, K. Laihem, and A. Schälicke, Nucl. Inst. Meth. A **559**, 185 (2006).
[19] J. Dumas, J. Grames, and E. Voutier, AIP Conf. Proc. **1160**, 120 (2009).